

Magnetocaloric effect in hexacyanochromate Prussian blue analogs

Espérance Manuel and Marco Evangelisti*

National Research Center on “nanoStructures and bioSystems at Surfaces” (S^3), INFM-CNR, 41100 Modena, Italy

Marco Affronte

National Research Center on “nanoStructures and bioSystems at Surfaces” (S^3), INFM-CNR,
and Dipartimento di Fisica, Università di Modena e Reggio Emilia, 41100 Modena, Italy

Masashi Okubo, Cyrille Train, and Michel Verdaguer

Chimie Inorganique et Matériaux Moléculaires, Unité CNRS 7071,
Université Pierre et Marie Curie, 75252 Paris, France

(Dated: September 30, 2018)

We report on the magnetocaloric properties of two molecule-based hexacyanochromate Prussian blue analogs, nominally $\text{CsNi}^{II}[\text{Cr}^{III}(\text{CN})_6] \cdot (\text{H}_2\text{O})$ and $\text{Cr}_3^{II}[\text{Cr}^{III}(\text{CN})_6]_2 \cdot 12(\text{H}_2\text{O})$. The former orders ferromagnetically below $T_C \simeq 90$ K, whereas the latter is a ferrimagnet below $T_C \simeq 230$ K. For both, we find significantly large magnetic entropy changes ΔS_m associated to the magnetic phase transitions. Notably, our studies represent the first attempt to look at molecule-based materials in terms of the magnetocaloric effect for temperatures well above the liquid helium range.

PACS numbers: 75.30.Sg, 75.40.Cx

Recent experiments^{1,2,3,4,5} have proven that molecule-based magnetic materials can manifest a significant magnetocaloric effect (MCE) that, in some cases,^{4,5} is even larger than for intermetallic and lanthanide-alloys conventionally studied and employed for cooling applications.⁶ This is certain for molecular compounds based on high-spin clusters with vanishing magnetic anisotropy for which the net cluster spins, resulting from strong intracluster superexchange interactions, are easily polarized by the applied-field providing large magnetic entropy changes ΔS_m . Their maximum efficiency in terms of MCE takes place, however, at liquid-helium temperatures. A possible solution to increase the temperature of the maximum ΔS_m is by considering larger anisotropies, although the drawback is that the entropy change gets smaller with increasing anisotropy.⁷ An alternative route to follow is to strengthen the intermolecular magnetic correlations which ultimately will give rise to long-range magnetic order (LRMO). The response to the application or removal of magnetic fields is indeed maximized near the magnetic ordering temperature. In this respect, extended molecule-based systems like Prussian blue analogs are particularly appealing since LRMO temperatures up to room temperature have been reported for this class of compounds.⁸

In this Brief Report we report a study of MCE on two Prussian blue analogs, nominally $\text{CsNi}^{II}[\text{Cr}^{III}(\text{CN})_6] \cdot (\text{H}_2\text{O})$ and $\text{Cr}_3^{II}[\text{Cr}^{III}(\text{CN})_6]_2 \cdot 12(\text{H}_2\text{O})$ (hereafter denoted as NiCr and Cr_3Cr_2 , respectively), showing different magnetic ordering at relatively high temperatures. Indeed, NiCr is known to undergo a transition to a long-range *ferromagnetic* ordered state at $\simeq 90$ K,⁹ whereas Cr_3Cr_2 behaves as a long-range ordered *ferrimagnet* at temperatures below $\simeq 230$ K.¹⁰ Both compounds crystallize in a cubic lattice,¹¹ the conventional unit cell is depicted in Fig. 1. Exchange coupling between the two

metallic center is ensured by the cyano-bridge. For NiCr, half of the tetrahedral interstitial sites are occupied by cesium atoms which maintain charge neutrality. Further information on the structure together with a description of the method of synthesis can be found in Refs.⁹ and ¹⁰ for NiCr and Cr_3Cr_2 , respectively. Susceptibility, magnetization and heat capacity measurements down to 2 K were carried out in a Quantum Design PPMS set-up for the $0 < H < 7$ T magnetic field range. All data were collected on powdered samples of the compounds.

For both compounds, Figure 2 shows the real component $\chi'(T)$ of the complex susceptibility collected with an ac-field $h_{ac} = 10$ G at $f = 1730$ Hz. For NiCr, the abrupt change of $\chi(T)$ at $T_C \simeq 90$ K is ascribed to the transition to a ferromagnetically ordered state, in which demagnetization effects become important. In

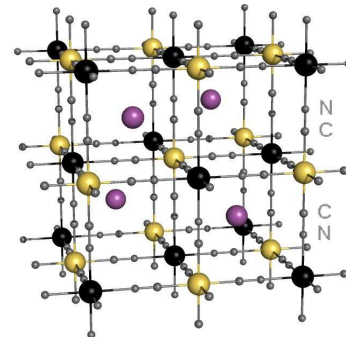


FIG. 1: (Color online). Sketch of a bimetallic Prussian blue analog. At the vertices, black spheres represent Cr^{III} ($s = 3/2$), whereas lighter-colored spheres represent either Ni^{II} (spin $s = 1$) or Cr^{II} ($s = 2$) atoms. Depicted as well are the Cs atoms at the interstitial sites (only relevant for the NiCr compound).

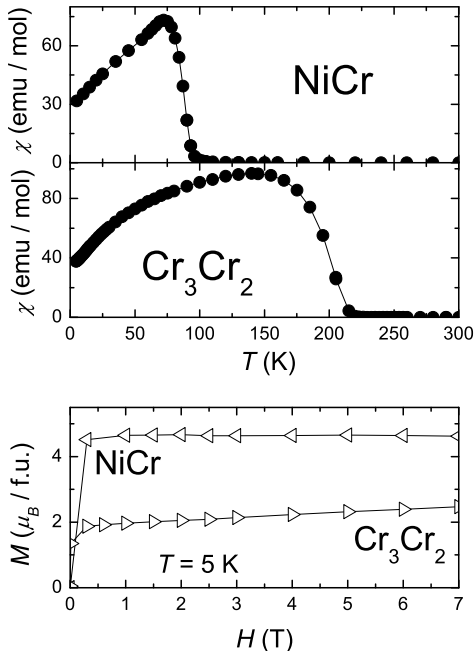


FIG. 2: Top: Real component of the molar ac-susceptibility $\chi(T)$, collected at $f = 1730$ Hz and ac-field $h_{ac} = 10$ G, for NiCr and Cr_3Cr_2 , as labeled. Bottom: Isothermal magnetization $M(H)$ of both NiCr and Cr_3Cr_2 for $T = 5$ K.

fact, the value of 73.5 emu/mol reached by $\chi(T)$ at T_C is of the same order as expected for an isotropic NiCr sample at the maximum.¹² In the linear regime of the inverse susceptibility corrected for the demagnetizing field, the fit to the Curie-Weiss law provides the Curie constant $C = 3.2$ emuK/mol and the Weiss constant $\theta = 118$ K, in agreement with the observed ferromagnetic ordering. The constant C is reasonably well accounted for by the expected value of randomly oriented spins that amounts to 3.1 emuK/mol, assuming $g = 2.2$ for Ni^{II} and $g = 2$ for Cr^{III} ions. In the ordered phase the saturation magnetization amounts to $4.6 \mu_B$ (Fig. 2), which corroborates the tendency of the Ni^{II} and Cr^{III} spins to align parallel. For Cr_3Cr_2 , the transition to the expected long-range ferromagnetically ordered state is observed at $T_C \approx 230$ K¹³ (Fig. 2). However, $\chi(T)$ does not reach its maximum at T_C but only at much lower temperatures (≈ 140 K), and then it decreases down by lowering T . The molar magnetization of Cr_3Cr_2 collected for $T = 5$ K increases sharply up to $\approx 1.9 \mu_B$ at $H = 0.3$ T and then follows a linear dependence with increasing field, reaching $\approx 2.5 \mu_B$ at $H = 7$ T (Fig. 2). As observed by Mallah *et al.*,¹⁰ the magnetization fails to reach the saturation value ($6 \mu_B$) expected for a full antiparallel alignment of the Cr^{II} and Cr^{III} spins. There are two possible reasons for this behavior: (i) Cr^{II} ions can also be in the low-spin state for which $s = 1$, instead of $s = 2$; (ii) the mag-

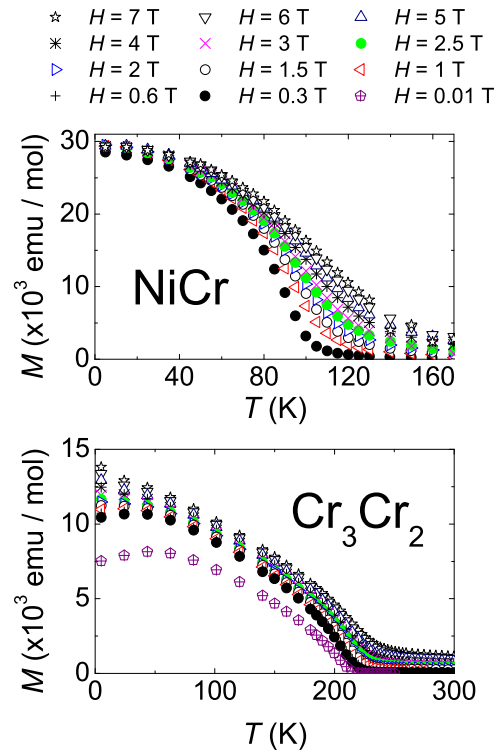


FIG. 3: (Color online). Field-cooled $M(T)$ curves measured at different applied-fields for NiCr (top) and Cr_3Cr_2 (bottom).

netic ordered structure is more complex than a simple ferrimagnet, and spin-canting or reorientation may take place in the ordered state accounting for the anomalous $\chi(T)$ dependence as well. The latter may be favored by the intrinsic $\text{Cr}^{II}(\text{CN})_6$ vacancies. Likely both reasons coexists, a large fraction of low-spin Cr^{II} would induce structural as well as magnetic disorder. We refrain from pushing any further the analysis since we do not have enough experimental information, because our measurements are performed on powder samples.

For a proper evaluation of the MCE of these compounds,¹⁴ we performed systematic magnetization $M(T, H)$ measurements as a function of temperature and field. Field-cooled $M(T, H)$ measurements for several applied-fields H up to 7 T show spontaneous magnetization below the corresponding T_C 's (Fig. 3). In an isothermal process of magnetization, the magnetic entropy change ΔS_m can be derived from Maxwell relations by integrating over the magnetic field change $\Delta H = H_f - H_i$, that is:

$$\Delta S_m(T)_{\Delta H} = \int_{H_i}^{H_f} \frac{\partial M(T, H)}{\partial T} dH. \quad (1)$$

From $M(H)$ data of Fig. 3, the obtained $\Delta S_m(T)$ for several ΔH values¹⁵ are depicted in Fig. 4. It can be seen that, for both compounds, ΔS_m has max-

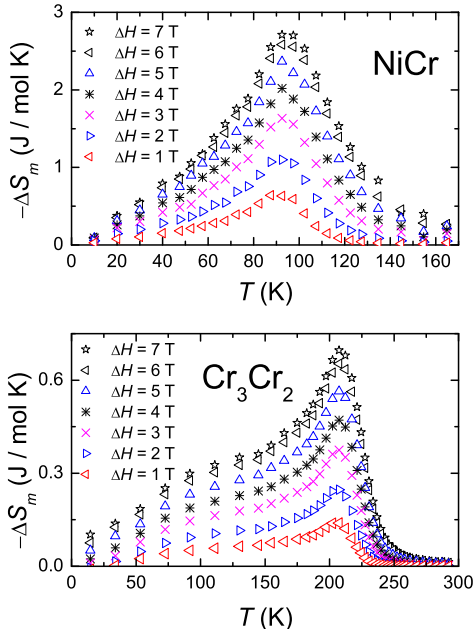


FIG. 4: (Color online). Magnetic entropy change $\Delta S_m(T)$ as obtained from $M(T, H)$ data of Fig. 3 for NiCr (top) and Cr_3Cr_2 (bottom), for several field changes ΔH , as labeled.

ima at temperatures corresponding that of the ordering temperatures. Interestingly, $\Delta S_m(T)$ of Cr_3Cr_2 keeps relatively large values for a broad T -range down to temperatures well below T_C . Moreover, we note that ΔS_m increases by increasing ΔH , reaching for $\Delta H = 7$ T the largest values of $2.8 \text{ J mol}^{-1}\text{K}^{-1}$ for NiCr and $0.70 \text{ J mol}^{-1}\text{K}^{-1}$ for Cr_3Cr_2 , or equivalently $6.6 \text{ J kg}^{-1}\text{K}^{-1}$ and $0.93 \text{ J kg}^{-1}\text{K}^{-1}$ for the former and the latter, respectively.

The magnetocaloric effect of a given magnetic material can be also evaluated from specific heat C/R measurements.¹⁴ The experimental specific heat of NiCr is displayed in Fig. 5 for $H = 0$ and $H = 7$ T. A careful look at the zero-field curve reveals the onset of the ferromagnetic phase transition at $T_C = 90$ K, corroborating the magnetization experiments. It can also be noticed that this contribution disappears upon application of the magnetic field, proving its magnetic origin. The magnetic contribution is hardly detectable, the reason is that, at the temperature region of the phase transition, the dominant contribution arises from thermal vibrations of the lattice.

In order to evaluate MCE from the $C(T, H)$ data of Fig. 5, we first determine the total entropies for $H = 0$ and 7 T as functions of T , according to

$$S(T)_H = \int_0^T \frac{C(T)_H}{T} dT. \quad (2)$$

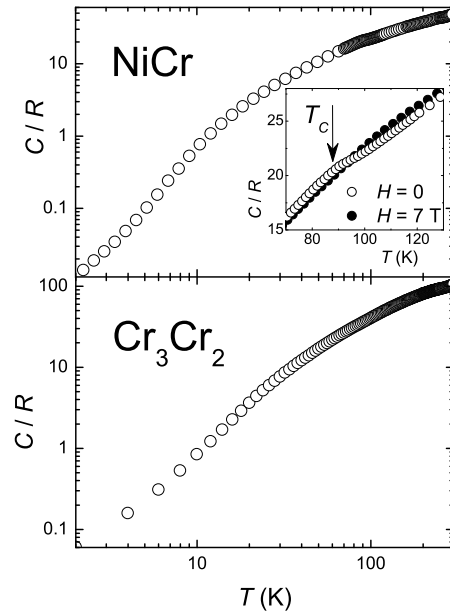


FIG. 5: Temperature dependence of the specific heat of NiCr (top) and Cr_3Cr_2 (bottom) collected for zero-applied-field. Top inset: Magnification of the region around the ferromagnetic ordering temperature $T_C \simeq 90$ K, for $H = 0$ and $H = 7$ T.

Experimental entropies are obtained integrating down to the lowest achieved $T \approx 2$ K and, obviously, not from $T = 0$ K as in principle required. However, this does not represent an obstacle for our purposes because at these temperatures the system is fully magnetically ordered and the magnetic entropy is therefore vanishingly small. For $\Delta H = (7 - 0)$ T, we then calculate the magnetic entropy change ΔS_m as well as the adiabatic temperature change ΔT_{ad} ,¹⁴ both as function of temperature. Note that the estimation of the lattice contribution is irrelevant for our calculations, since we deal with differences between total entropies at different H . The results obtained for ΔS_m and ΔT_{ad} are displayed in Fig. 6. The largest changes are seen near T_C , where we get $-\Delta S_m = (2.5 \pm 0.3) \text{ J mol}^{-1}\text{K}^{-1}$, or equivalently $(5.9 \pm 0.7) \text{ J kg}^{-1}\text{K}^{-1}$, and $\Delta T_{ad} = (1.2 \pm 0.1) \text{ K}$. It can be noticed that the obtained ΔS_m agrees with the previous estimate inferred from $M(T, H)$, suggesting that both independent procedures can be effectively used to characterize the NiCr compound with respect to its magnetocaloric properties.

As for NiCr and for the sake of completeness, we performed heat capacity experiments for Cr_3Cr_2 as well. However, one has to consider that for this system we expect ferrimagnetic order at $T_C \simeq 230$ K. The resulting magnetic moment per formula unit is rather small (Fig. 2), especially taking into account the large lattice contribution that takes place at these very high temper-

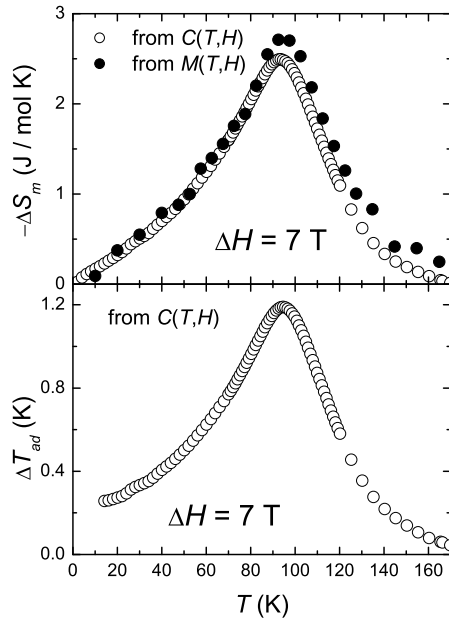


FIG. 6: For NiCr. Top: $\Delta S_m(T)$ as obtained from C (empty dots) and M data (filled dots), both for $\Delta H = 7$ T. Bottom: $\Delta T_{ad}(T)$ as obtained from C data, for $\Delta H = 7$ T.

atures. It is therefore not surprising that no magnetic anomaly is detectable in the $C(T, H)$ curves. The lower

panel of Fig. 5 shows indeed the measured curve, which essentially does not depend on the applied-field.

Summing up the experimental results here presented, the magnetocaloric response for the molecular materials NiCr and Cr_3Cr_2 shows maximum entropy changes near the ordering temperatures, 90 and 230 K, respectively. This places the two Prussian blue analogs in a temperature range still below room temperature, which is dominated, with reference to MCE variations, by lanthanide-based materials.¹⁶ As a matter of fact, a direct comparison reveals that the NiCr and Cr_3Cr_2 compounds have ΔS_m and ΔT_{ad} that are about an order of magnitude smaller. In spite of such a large gap, our results are encouraging since they represent a strong improvement with respect to the molecule-based materials investigated so far in terms of MCE, for which large MCE variations take place only below 10 K.^{1,2,3,4,5} The relevant point is that, as for conventional materials investigated and proposed for cooling applications,⁶ the mechanism of magnetic ordering can be efficiently exploited also in this class of materials to enhance the magnetocaloric effect.

This work is partially funded by the Italian MIUR under FIRB project No. RBNE01YLKN and by the EC-Network of Excellence “MAGMANet” (No. 515767). E.M. was supported by a fellowship from the EC-Marie Curie network “QuEMolNa” (No. MRTN-CT-2003-504880). M.O was supported by Research Fellowships of the Japan Society for the Promotion of Science for Young Scientists.

* Corresponding author.

Electronic address: evange@unimore.it

¹ F. Torres, J.M. Hernández, X. Bohigas, and J. Tejada, *Appl. Phys. Lett.* **77**, 3248 (2000).

² F. Torres, X. Bohigas, J.M. Hernández, and J. Tejada, *J. Phys.: Condens. Matter* **15**, L119 (2003).

³ M. Affronte, A. Ghirri, S. Carretta, G. Amoretti, S. Piligkos, G.A. Timco, and R.E.P. Winpenny, *Appl. Phys. Lett.* **84**, 3468 (2004).

⁴ M. Evangelisti, A. Candini, A. Ghirri, M. Affronte, E.K. Brechin, and E.J.L. McInnes, *Appl. Phys. Lett.* **87**, 072504 (2005).

⁵ M. Evangelisti, A. Candini, A. Ghirri, M. Affronte, S. Piligkos, E.K. Brechin, and E.J.L. McInnes, *Polyhedron* **24**, 2573 (2005).

⁶ see, i.e., K.A. Gschneidner Jr., V.K. Pecharsky and A.O. Tsokol, *Rep. Prog. Phys.* **68**, 1479 (2005), and references therein.

⁷ X.X. Zhang, H.L. Wei, Z.Q. Zhang, and L.Y. Zhang, *Phys. Rev. Lett.* **87**, 157203 (2001).

⁸ see, i.e., M. Verdaguer and G. Girolami, *Magnetic Prussian blue analogs in Magnetism: Molecules to Materials V*, Edited by J.S. Miller and M. Drillon (Wiley-VCH Verlag GmbH & Co. KGaA, Weinheim, 2004).

⁹ V. Gadet, T. Mallah, I. Castro, and M. Verdaguer, *J. Am.*

Chem. Soc. **114**, 9213 (1992).

¹⁰ T. Mallah, S. Thiébaud, M. Verdaguer, and P. Veillet, *Science* **262**, 1554 (1993).

¹¹ For NiCr, the cell parameter is $a = 10.50$ Å and the molecular weight is $m_w = 424.4$ g. For Cr_3Cr_2 , $a = 10.39$ Å and $m_w = 788.3$ g.

¹² An estimate of the demagnetizing factor ($N \approx 0.6$) gives the value of ≈ 91 emu/mol for the susceptibility of an isotropic ferromagnetic NiCr sample at the maximum, assuming a cylindrical approximation of its shape.

¹³ The observed ordering temperature of Cr_3Cr_2 slightly differs from that reported in Ref.¹⁰. The small discrepancy can be explained by the water content: 12(H_2O) here vs. 10(H_2O) in Ref.¹⁰. It is known indeed that the amount of water may (i) vary from sample to sample, (ii) affect the magnetic properties.⁸

¹⁴ V.K. Pecharsky and K.A. Gschneidner Jr., *J. Appl. Phys.* **86**, 565 (1999).

¹⁵ For practical reasons, the measurements at the lowest applied field were carried out for $H_i = 10^{-3}$ T, which in our calculations was approximated to zero-applied-field.

¹⁶ see, i.e., V.K. Pecharsky and K.A. Gschneidner Jr., *J. Magn. Mater.* **200**, 44 (1999), and references therein.